JB
Journals.ASM.org

A λ Cro-Like Repressor Is Essential for the Induction of Conjugative Transfer of SXT/R391 Elements in Response to DNA Damage

Dominic Poulin-Laprade, Vincent Burrus

Laboratory of Bacterial Molecular Genetics, Département de Biologie, Faculté des Sciences, Université de Sherbrooke, Sherbrooke, Québec, Canada

ABSTRACT

Integrative and conjugative elements (ICEs) of the SXT/R391 family are the main contributors to acquired multidrug resistance in the seventh pandemic lineage of *Vibrio cholerae*, the etiological agent of the diarrheal disease cholera. Conjugative transfer of SXT/R391 ICEs is triggered by antibiotics and agents promoting DNA damage through RecA-dependent autoproteolysis of SetR, an ICE-encoded λ CI-like repressor. Here, we describe the role of CroS, a distant λ Cro homolog, as a key component contributing to the regulation of expression of the activator SetCD that orchestrates the expression of the conjugative transfer genes. We show that deletion of *croS* abolishes the SOS response-dependent induction of SXT despite the presence of a functional *setR* gene. Using quantitative reverse transcription-PCR and *lacZ* reporter assays, we also show that CroS represses *setR* and *setCD* expression by binding to operator sites shared with SetR. Furthermore, we provide evidence of an additional operator site bound by SetR and CroS. Finally, we show that SetCD expression generates a positive feedback loop due to SXT excision and replication in a fraction of the cell population. Together, these results refine our understanding of the genetic regulation governing the propagation of major vectors of multidrug resistance.

IMPORTANCE

Healthcare systems worldwide are challenged by an alarming drug resistance crisis caused by the massive and rapid propagation of antibiotic resistance genes and the associated emergence of multidrug-resistant pathogenic bacteria. SXT/R391 ICEs contribute to this phenomenon not only in clinical and environmental vibrios but also in several members of the family *Enterobacteriaceae*. We have identified and characterized here the regulator CroS as a key factor in the stimulation of conjugative transfer of these ICEs in response to DNA-damaging agents. We have also untangled conflicting evidence regarding autoactivation of transfer by the master activator of SXT/R391 ICEs, SetCD. Discovery of CroS provides a clearer and more complete understanding of the regulatory network that governs the dissemination of SXT/R391 ICEs in bacterial populations.

Cholera is a severe infectious disease caused by the ingestion of food or water contaminated by *Vibrio cholerae*. This disease remains widespread in regions with limited access to clean water and where poor sanitation allows easy dissemination of the bacterium in drinking water sources. Cholera is characterized by a profuse watery diarrhea that rapidly induces massive fluid loss, causing severe dehydration of the patient, which may lead to death within 24 h of symptom onset. Although epidemic cholera is usually caused by *V. cholerae* O1, the unusual serogroup O139 emerged in the early 1990s as the cause of a cholera outbreak in India (1). O139 clinical isolates were found to be resistant to sulfamethoxazole and trimethoprim, two antibiotics commonly used for the treatment of severe cases of cholera (2). This resistance was found to be transmissible and linked to an integrative and conjugative element (ICE) named SXT (3). ICEs are self-transmissible bacterial mobile elements that play a major role in gene exchange in bacterial populations, as they are horizontally transferred via conjugation by a process similar to that used by many conjugative plasmids (4, 5). Unlike plasmids, ICEs do not remain stably in an episomal form and are rather found integrated into the chromosome. SXT integrates itself into the chromosome of *V. cholerae* in a site-specific manner at the 5′ end of *prfC*, a gene coding for the peptide release factor RF3 (6). Since the discovery of SXT, SXT or related ICEs have been found to be prevalent in the seventh pandemic isolates of *V. cholerae* and sporadically present in other *Vibrio* species (7–9) and other *Gammaproteobacteria* of clinical origin or isolated from the aquatic environment, such as *Photobacterium* (10), *Proteus* (11), *Alteromonas* (12), *Marinomonas* (13), and *Shewanella* (9, 14) species. SXT is closely related to R391, an ICE conferring resistance to kanamycin and mercury, originally detected in a 1967 South African isolate of *Providencia rettgeri* (15, 16). All of the ICEs related to SXT and R391 are grouped into a single family, namely, the SXT/R391 family, because they all have the same chromosomal integration site and a set of conserved genes essential for site-specific integration, conjugative transfer, and regulation (6, 8). SXT/R391 ICEs also contain variable DNA insertions conferring adaptive traits, including resistance to antibiotics, heavy metals, and bacteriophage infection (8, 17, 18); synthesis of the second messenger c-di-GMP (19); and homologous recombination and mutagenic repair systems (20, 21). Beside their own transfer, SXT/R391 ICEs have been shown to mobilize plasmids, phylogenetically unrelated genomic

Received 31 July 2015 **Accepted** 26 September 2015

Accepted manuscript posted online 5 October 2015

Citation Poulin-Laprade D, Burrus V. 2015. A λ Cro-like repressor is essential for the induction of conjugative transfer of SXT/R391 elements in response to DNA damage. J Bacteriol 197:3822–3833. doi:10.1128/JB.00638-15.

Editor: R. L. Gourse

Address correspondence to Vincent Burrus, Vincent.Burrus@USherbrooke.ca.

Supplemental material for this article may be found at http://dx.doi.org/10.1128/JB.00638-15.

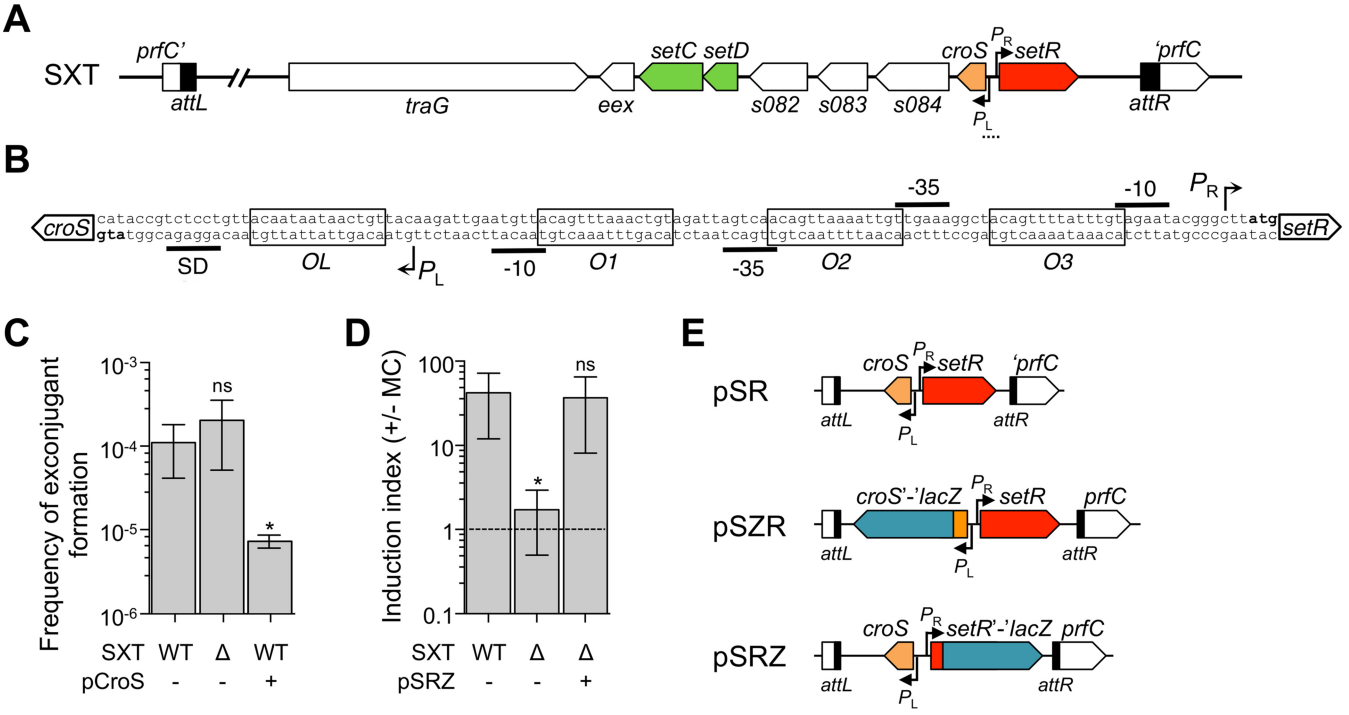

FIG 1 Effects of *croS* on SXT conjugative transfer. (A) Schematic representation of the regulatory module of SXT. The dotted line indicates the region enlarged in panel B. (B) The intergenic region between *croS*, previously referred to as *s086*, and *setR* in SXT as represented by Beaber and Waldor (30). The P_L and P_R promoters, the OL, O1, O2, and O3 operators, the −10 and −35 elements, the Shine-Dalgarno (SD) sequence of *croS*, and the start codons of *croS* and *setR* are represented. (C) Effect of the deletion or overexpression of *croS* on SXT transfer. Conjugation assays were carried out with *E. coli* BW25113 SXT (VB17, WT) or its Δ*croS* mutant (DPL353, Δ) as the donor. Overexpression assays were carried out by expressing *croS* from the arabinose-inducible P_{BAD} promoter in pCroS (DPL525). *E. coli* CAG18439 (Tc^r) was used as the recipient. Frequencies of exconjugant formation were expressed as the number of exconjugant CFU (Su^r Tm^r Tc^r) per recipient CFU (Tc^r). (D) Effect of *croS* deletion on the induction of SXT transfer by MC. The donor strains were VB17, DPL353, and DPL263 in which *croS* was expressed from its native P_L promoter in pSRZ integrated in single copy in tandem with SXT Δ*croS*. The recipient strain was CAG18439. The induction index corresponds to the ratio of the frequencies of exconjugant formation obtained with and without MC treatment prior to transfer. The dashed line indicates an induction index of 1, i.e., no difference between the induced and noninduced conditions. Each bar represents the mean and standard deviation of values obtained from at least three independent experiments. Statistical analyses of the logarithms of the mean values were performed with two-tailed unpaired *t* tests. Asterisks indicate that *P* values are <0.05 compared to the wild type (WT). (E) Schematic representation of the insert of the pSR, pSZR, and pSRZ plasmids site specifically integrated into the 5′ end of *prfC* alone or in tandem with SXT. The plasmid backbone is not represented. In pSZR and pSRZ, *lacZ* was translationally fused to the sixth codon of *croS* and *setR*, respectively.

islands (mobilizable genomic islands), and up to 1.5 Mb of chromosomal DNA by high-frequency recombination transfer (22, 23).

The most conserved genes (97% identity at the nucleotide level) shared by SXT/R391 ICEs are *s086* and *setR*, which belong to the regulatory module located at the rightmost end of the integrated ICE, near the *attR* attachment site (Fig. 1A) (8). The regulatory module contains eight open reading frames (ORFs), seven of which are in the same orientation (*s086*, *s084*, *s083*, *s082*, *setD*, *setC*, and *eex*), while the last gene, *setR*, is divergently transcribed (Fig. 1A and B) (24). *eex* and the convergent gene *traG* code for the entry exclusion system of SXT/R391 ICEs (25). The overlapping genes *setC* and *setD* encode the SetCD activator complex. SetCD was shown to bind upstream of the −35 sequence of 11 promoters in SXT/R391 ICEs, activating the expression of >40 genes essential for site-specific and homologous recombination, ICE replication and partition, and conjugative transfer (26–28). The functions of *s082*, *s083*, *s084*, and *s086* remain unknown. *In silico* analysis has revealed that *s086* codes for a putative small basic protein of 9.4 kDa with a predicted helix-turn-helix (HTH) DNA-binding domain. *setR* codes for the main repressor of SXT/R391 ICEs (24, 29). SetR contains an HTH_XRE (PF01381) motif in its N-terminal moiety and a C-terminal LexA-like autoproteolysis domain (PF00717). SetR is related to phage 434 CI and other lambdoid phage repressors and has been shown to bind to four operator sites located between *s086* and *setR* (Fig. 1B) (24, 30). These operators, O1, O2, O3, and OL, are part of P_L and P_R, two divergent overlapping promoters located in the intergenic region between *s086* and *setR*. The relative affinities of SetR for these four operator sites and their positions suggest an autoregulation of *setR* expression from P_R (30) and a repression of the operon containing *s086* and *setCD* driven from P_L (29). Repression at P_L is alleviated when the cellular pool of SetR drops, most likely as a result of autoproteolysis stimulated by DNA damage-induced activation of RecA (29).

The relative positions of *setR* and *s086* are reminiscent of *cI* and *cro* carried by bacteriophage λ. CI and Cro form a pair that governs the transition between the lysogenic and lytic pathways of the λ life cycle (31, 32). To date, SXT/R391 ICEs have been known to be regulated by only two transcriptional regulators, the repressor SetR and the activator complex SetCD (24). In this study, we identify S086 as a third regulator, which will be referred to as CroS for Cro-like repressor of SXT. We demonstrate that CroS is a key factor in the alleviation of SetR repression and induction of con-

TABLE 1 Strains and plasmids used in this study

Strain or plasmid	Relevant genotype or description (phenotype)[a]	Reference(s) or source
E. coli strains		
CAG18439	MG1655 *lacZU118 lacI42*::Tn*10* (Tc^r)	76
HW220	CAG18439 *prfC*::SXT (Su^r Tm^r)	6
DC147	CAG18439 *prfC*::SXT Δ*traI*::*aph* (Su^r Tm^r Kn^r)	This study
BW25113	F^- Δ(*araD-araB*)*567* Δ*lacZ4787*(::*rrnB-3*) λ^- *rph-1* Δ(*rhaD-rhaB*)*568 hsdR514*	37, 77
β2163	(F^-) RP4-2-Tc::Mu Δ*dapA*::(*erm-pir*) (Kn^r Em^r)	36
BL21(DE3)	F^- *ompT* Δ*hsdS gal dcm* λDE3	Novagen
VB17	BW25113 *prfC*::SXT (Su^r Tm^r)	28
DPL353	BW25113 *prfC*::SXT Δ*croS* (Su^r Tm^r)	This study
DPL263	BW25113 *prfC*::[SXT Δ*croS*]-pSRZ (Su^r Tm^r Cm^r)	This study
DPL525	BW25113 *prfC*::SXT pCroS (Su^r Tm^r Ap^r)	This study
DPL297	BW25113 *prfC*::SXT *setD′-′lacZ-aad7* Δ*setC* (Su^r Tm^r Sp^r)	This study
DPL548	BW25113 *prfC*::[SXT Δ*traI*::*aph setD′-′lacZ-aad7* Δ*setC*] (Su^r Tm^r Sp^r Kn^r)	This study
DPL231	BW25113 *prfC*::pSR (*croS-setR*) (Su^r Tm^r)	This study
DPL241	BW25113 *prfC*::pSZR (*croS′-′lacZ-setR*) (Su^r Tm^r)	This study
DPL246	BW25113 *prfC*::pSRZ (*croS-setR′-′lacZ*) (Su^r Tm^r)	This study
Plasmids		
pVI36	PCR template for one-step chromosomal gene inactivation (Sp^r)	78
pKD13	PCR template for one-step chromosomal gene inactivation (Kn^r)	37
pVI42B	pVI36 BamHI::P_{lac}-*lacZ* (Sp^r)	20
pKD46	λRed recombination arabinose-inducible encoding plasmid (Ap^r)	37
pSW23T	$oriT_{RP4}$ $oriV_{R6K\gamma}$ (Cm^r)	36
pSR	pSW23T *croS-setR* $attP_{SXT}$ (Cm^r)	This study
pSZR	pSW23T *croS′-′lacZ-aad7-setR* $attP_{SXT}$ (Sp^r Cm^r)	This study
pSRZ	pSW23T *croS-setR′-′lacZ-aad7* $attP_{SXT}$ (Sp^r Cm^r)	This study
pVI68	pAH57 Δ(xis_λ-int_λ)::int_{SXT} (Ts)	20
pBAD-TOPO	ori_{pBR322} *bla araC* P_{BAD} (Ap^r)	Invitrogen
pBAD30	ori_{p15A} *bla araC* P_{BAD} (Ap^r)	79
pGG2B	pBAD30::*setDC* (Ap^r)	28
pCroS	pBAD-TOPO::*croS* (5′-3′) (Ap^r)	This study
pCroS-inv	pBAD-TOPO::*croS* (3′-5′) (Ap^r)	This study
pSetR	pBAD-TOPO::*setR* (Ap^r)	This study
pTraI	pBAD-TOPO::*traI* (Ap^r)	27
pCR2.1-TOPO	ori_{pUC} (Ap^r Kn^r)	Invitrogen
pDPL128	pCR2.1-TOPO::P_L-P_R (Ap^r Kn^r)	This study
pGEX-croS	pGEX-6P-1::*croS* (Ap^r)	This study
pGEX-setR	pGEX-6P-1::*setR* (Ap^r)	This study

[a] Ap^r, ampicillin resistant; Cm^r, chloramphenicol resistant; Em^r, erythromycin resistant; Kn^r, kanamycin resistant; Sp^r, spectinomycin resistant; Su^r, sulfamethoxazole resistant; Tc^r, tetracycline resistant; Tm^r, trimethoprim resistant; Ts, thermosensitive.

jugative transfer of SXT/R391 ICEs. By binding to five operator sites shared with SetR, CroS acts as a repressor of P_L and P_R, thereby repressing both *setCD* and *setR* by a mechanism that is evocative of λ Cro repression on CI and CII (33). We also show that SetCD increases its own expression not by activating P_L but by indirectly generating a positive feedback loop triggered by activation of SXT replication, which increases the SXT copy number and ultimately the level of the *setCD* mRNA transcript. Finally, we propose a new model of SXT transfer regulation that includes CroS as a repressor of P_L and P_R, thereby promoting the SOS-dependent induction of SXT/R391 ICE transfer.

MATERIALS AND METHODS

Bacterial strains and media. The bacterial strains used in this study are described in Table 1. The strains were routinely grown in lysogeny broth (LB-Miller; EMD) at 37°C in an orbital shaker/incubator and maintained at −80°C in LB broth containing 15% (vol/vol) glycerol. Antibiotics were used at the following concentrations: ampicillin, 100 μg ml^{-1}; chloramphenicol, 20 μg ml^{-1}; erythromycin, 10 μg ml^{-1}; kanamycin, 50 μg ml^{-1}; spectinomycin, 50 μg ml^{-1}; sulfamethoxazole (Su), 160 μg ml^{-1}; tetracycline (Tc), 12 μg ml^{-1}; trimethoprim (Tm), 32 μg ml^{-1}. When required, bacterial cultures were supplemented with 0.1 mM isopropyl-β-D-thiogalactopyranoside (IPTG), 0.02% L-arabinose, or 100 ng ml^{-1} mitomycin C (MC).

Bacterial conjugations. Conjugation assays were performed as described by Burrus and Waldor (34), with the following modifications. When induction with MC was performed, overnight cultures of donor and recipient cells were diluted 1:4 and the donor cultures were supplemented or not with MC and incubated for 1 h at 37°C with shaking. The cells were harvested by centrifugation for 3 min at 1,200 × *g*, washed in 1 volume of LB broth, and resuspended in 1/20 volume of LB broth. Mating mixtures were then deposited on LB agar plates and incubated at 37°C for 2 h.

Molecular biology methods. Plasmid DNA was prepared with the EZ-10 Spin Column Plasmid DNA Minipreps kit (Bio Basic) according to the manufacturer's instructions. All of the enzymes used in this study were purchased from New England BioLabs. PCR assays were performed with the Taq, Q5, or Phusion polymerase according to the manufacturer's instructions. When necessary, PCR products were purified with an EZ-10

Spin Column PCR Products Purification kit (Bio Basic) according to the manufacturer's instructions. *E. coli* was transformed by electroporation as described by Dower et al. (35) in a Bio-Rad Gene Pulser Xcell apparatus set at 25 μF, 200 Ω, and 1.8 kV with 1-mm gap electroporation cuvettes. Sequencing reactions were performed by the Plateforme de Séquençage et de Génotypage du Centre de Recherche du CHUL (Québec, QC, Canada).

Plasmid and strain constructions. The plasmids and oligonucleotides used in this study are listed in Table 1 (also see Table S1 in the supplemental material). Plasmids pCroS and pSetR were constructed by amplifying *croS* and *setR* with primer pair s086pBADf/s086pBADr.s or setRpBADf/setRpBADr.s and genomic DNA of *E. coli* HW220 as the template and cloning into the TA cloning expression vector pBAD-TOPO (Invitrogen) according to the manufacturer's instructions. pSR was constructed by PCR amplification of the *croS-setR-attP* region resulting from the excision of SXT in *E. coli* HW220 with the primer pair PEs086/VISLR3. The 2,022-bp PCR product was first cloned into pCR2.1-TOPO (Invitrogen) according to the manufacturer's instructions. The cloned fragment was then recovered by NotI/BamHI digestion and then ligated to NotI/BamHI-digested pSW23T, yielding pSR. pSW23T contains the RP4 mobilization locus, the R6K *pir*-dependent conditional origin of replication, and a chloramphenicol resistance gene (36). Plasmid pDPL128 was constructed by cloning into pCR2.1-TOPO (Invitrogen) the intergenic region between *setR* and *croS*, which was amplified by PCR with primer pair RRs086-4/RRs086setRr and genomic DNA of *E. coli* HW220 as the template.

Δ*croS* and Δ*traI* mutant derivatives of SXT were constructed in *E. coli* HW220 by the one-step chromosomal gene inactivation technique (37) with primer pairs delS086F/dels086R and TraIWF2/TraIWR3, respectively, and the pKD13 template. SXT Δ*traI*::*aph* complemented with pTraI was transferred by conjugation into *E. coli* BW25113. To construct *E. coli* DPL548, the Δ*traI*::*aph* mutation was then transduced into *E. coli* DPL297 (BW25113 *prfC*::SXT Δ*setCD*::*lacZ-aad7*) by P1*vir* generalized transduction. Strains containing pSR integrated into the 5′ end of *prfC* were constructed by mating the RP4$^+$ *pir*$^+$ strain *E. coli* β2163/pSR with *E. coli* BW25113 containing pVI68 as the recipient strain. pVI68 expresses the integrase of SXT, thereby allowing site-specific integration of pSR, which was verified by amplifying the *attL* and *attR* sites by PCR with primer pairs EattBR/VISRF and EattBF/VISLR3, respectively. The absence of multiple integrations of pSR in tandem arrays was verified with primers VISLR3 and VISRF. The resulting strain, *E. coli* DPL231, contains a unique copy of the *croS-setR* region integrated site specifically into *prfC*. Translational *lacZ* fusions *setR′-′lacZ*, *croS′-′lacZ*, and *setCD′-′lacZ* were constructed by the one-step chromosomal gene inactivation technique (37) with primer pairs DATsetR-lacZf/DATsetR-lacZr, DATsetQ-lacZf/DATsetQ-lacZr, and DATsetCD-lacZf/DATsetCD-lacZr, respectively, and pVI42B as the template. In each construct, the sixth codon of the gene of interest was fused to the ninth codon of *lacZ*. The *setR′-′lacZ* and *croS′-′lacZ* mutations targeted BW25113 derivative strains containing pSR integrated into *prfC* (DPL231), whereas the *setCD′-′lacZ* mutation targeted SXT in *E. coli* VB17. SXT Δ*croS* was transferred into DPL246 by conjugation to generate DPL263.

RNA isolation and quantitative reverse transcription (qRT)-PCR. Total RNA was extracted and cDNA were synthesized as described previously (19, 38). RNA integrity was verified with a 2100 Bioanalyzer (Agilent). Quantitative amplification of *setR*, *croS*, *setD*, and *setC* was carried out with primer pairs RTsetR-F/RTsetR-R, RTcroS-F/RTcroS-R, RTsetD-F/RTsetD-R, and RTsetC-F/RTsetC-R, respectively. For normalization, *rpoZ* was amplified with primers RTrpoZcoli-F/RTrpoZcoli-R and the $\Delta\Delta C_T$ calculation method. Experiments were repeated three times in triplicate and combined. Melting curves were determined with the final reaction products (156 to 165 bp) to confirm that amplification was specific to targets. All primer pairs exhibited efficiencies between 95 and 97%.

Real-time qPCR assays for relative quantification of *attB* and *attP*. The frequency of excision and copy number of the excised circular form of SXT were assessed by real-time quantitative PCR (qPCR) as described elsewhere (39). Genomic DNA was obtained from cultures of *E. coli* VB17, DPL297/pGG2B, and DPL548/pGG2B cells grown under conditions described for the qRT-PCR assays. Bacterial cultures were grown in LB medium at 37°C to an optical density at 600 nm (OD_{600}) of 0.2 and then for an additional 2 h at 37°C. *prfC*, *attB*, and *attP* were quantified with primer pairs prfC.qec.F1/prfC.qec.R1, attB.qec.F2/attB.qec.R2, and attP.qec.F2/attP.qec.R2, respectively (27) (see Table S1 in the supplemental material). Three biological replicates of qPCR experiments were performed on the RNomics platform of the Laboratoire de Génomique Fonctionnelle de l'Université de Sherbrooke, Sherbrooke, QC, Canada (http://lgfus.ca). Normalization was performed as described previously (39).

β-Galactosidase assays. The substrate used to determine LacZ levels was *o*-nitrophenyl-β-D-galactopyranoside, and the assays were carried out as described previously (40) with LB medium and 100 μg ml^{-1} ampicillin for maintenance of pCroS and pGG2B. Induction of *croS* and *setCD* expression and of the SOS response was done by supplementing, respectively, with 0.2% arabinose and/or 100 ng ml^{-1} MC a refreshed culture grown to an OD_{600} of 0.2, followed by a 2-h incubation at 37°C with shaking prior to cell sampling.

Expression and purification of the SetR and CroS proteins. Overnight-grown cultures of *E. coli* BL21(DE3) bearing pGEX-croS or pGEX-setR were diluted 1/1,000 in fresh 2× YT broth (80) supplemented with 100 μg ml^{-1} ampicillin and incubated at 37°C with agitation. Protein expression was induced at mid-exponential phase (OD_{600} of 0.6) with 0.1 mM IPTG. The cultures were grown for an additional 3 h at 37°C with agitation. Cells were collected by centrifugation, resuspended in phosphate-buffered saline containing 1% Triton X-100, 1 mM phenylmethylsulfonyl fluoride, and a cocktail of protease inhibitors (Protease Inhibitor Cocktail; Sigma). Cells were lysed by sonication and centrifuged to pellet the debris, and CroS and SetR were recovered by affinity chromatography with the glutathione *S*-transferase purification module (GE Healthcare) and the PreScission protease (GE Healthcare) according to the manufacturer's instructions. Protein concentration was estimated with the Bradford protein assay (Bio-Rad), and purity was determined by SDS-PAGE analysis.

Dimerization assay. Prior to dimerization assay, the purity of CroS was estimated by SDS-PAGE analysis to be 95%. No contaminant proteins with a size similar to that of CroS was observed. A 4.7-μg sample of purified CroS was incubated with 0.625% glutaraldehyde for 30 min at room temperature. The reaction mixture was then denatured at 100°C for 3 min, loaded onto a 15% SDS-PAGE gel, and run for 75 min at 150 V (41). The gel was then stained with Coomassie brilliant blue R-250. The Precision Plus Protein Kaleidoscope Standards ladder (Bio-Rad) was used as a molecular weight marker.

EMSAs. The probes used in electrophoretic mobility shift assays (EMSAs) were either annealed oligonucleotides or PCR products. Purified PCR products and a single oligonucleotide for each annealed pair were labeled with [γ-^{32}P]dATP with the T4 polynucleotide kinase. An equimolar quantity of the complementary oligonucleotide was added, the volume was brought to 100 μl in 20 mM Tris-HCl (pH 8.0)–20 mM KCl, and the mixture was denatured at 95°C for 5 min and then cooled to room temperature over 1 h. The γ-^{32}P-labeled double-stranded DNA fragments were separated from unincorporated [γ-^{32}P]dATP with Illustra Micro Spin G-25 columns (GE Healthcare) according to the manufacturer's instructions. Purified CroS and SetR proteins were preincubated in 24 μl of buffer I (20 mM Tris-HCl [pH 8.0], 20 mM KCl, 1 mM $MgCl_2$, 5% glycerol) for 20 min at 4°C. For PCR probes 1 to 6 (Fig. 4D), nonspecific competitor DNA was added by supplementing buffer I with sonicated salmon sperm DNA at 50 ng ml^{-1}. Radiolabeled probes (2,000 cpm) were added, and samples were incubated for 30 min at 37°C and then for 10 min at 4°C. Samples were immediately loaded onto a prerun 4% polyacrylamide gel containing 0.5× Tris-borate-EDTA buffer and subjected to electrophoresis at a constant voltage of 120 V at 4°C for 1 h 15 min. Gels were dried and exposed to a Phosphor Screen (Kodak), and results were visualized with a Typhoon FLA 9500 imager (GE Healthcare). The densi-

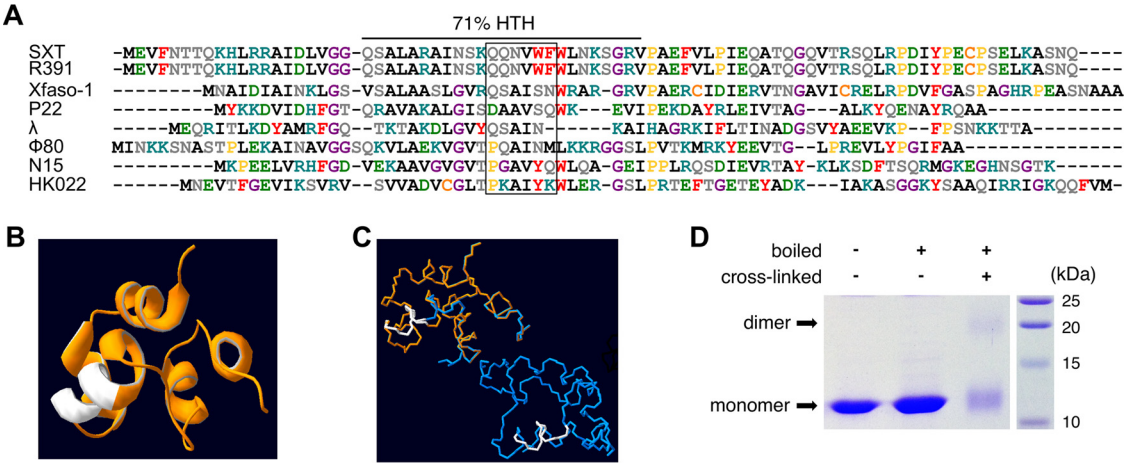

FIG 2 Predicted structure and DNA-binding domain of CroS. (A) Amino acid sequence alignment of Cro-like repressors computed by Clustal Omega (72). The source ICE or phage is indicated on the left. Sequences are sorted according to phylogenetic proximity. Amino acids are color coded as follows according to their chemical properties: pink, positively charged; green, negatively charged; gray, no charge, polar, and hydrophilic; red, aromatic; black, hydrophobic; orange, cysteine; yellow, proline; purple, glycine. DNA recognition helices as described by Hall et al. (43) are indicated by a black box. The Dodd and Egan method predicted a 71% chance of an HTH motif (73). (B) Three-dimensional ribbon structure of CroS as modeled by Phyre2 with template Protein Data Bank (PDB) entry 3BD1 (Cro protein from Xfaso 1 in *X. fastidiosa* strain ann-1) with 99.9% confidence, 76% coverage, and 38% identity (44). The putative DNA recognition helix is shown in white. (C) Superposition of the modeled monomer of CroS (orange) and a dimer of Xfaso 1 (blue) as crystallized by Roessler et al. (42) with the predicted DNA recognition helices shown in white. (D) SDS-PAGE analysis of purified CroS protein cross-linked or not with 0.625% glutaraldehyde.

tometry values (intensity units per millimeter squared) of each shifted operator were quantified with the Quantity One software (Bio-Rad). The background was subtracted, and then percentages of maximal intensity were calculated by dividing the density of each band by the highest density, both obtained with 1 μM SetR or CroS.

DNase I protection assays. To analyze the top strand, the probe was prepared first by digesting pDPL128 with HindIII. The linearized plasmid was then dephosphorylated with Antarctic phosphatase and subsequently digested with NsiI. To analyze the bottom strand, the probe was prepared by digestion of pDPL128 with XhoI, Antarctic phosphatase dephosphorylation, and digestion with KpnI. The probes were then end labeled with the T4 polynucleotide kinase and [γ-^{32}P]ATP at 6,000 Ci mmol^{-1}. Fifty-microliter binding reaction mixtures containing CroS and the radiolabeled probe (20,000 cpm) were prepared as described for EMSAs. Fifty microliters of cofactor solution (10 mM $MgCl_2$, 5 mM $CaCl_2$) and 0.1 U of DNase I were added, and the mixture was incubated for 2 min at room temperature. The reaction was terminated by the addition of 100 μl of stop solution (1% SDS, 200 mM NaCl, 20 mM EDTA [pH 8.0], tRNA at 40 μg ml^{-1}) and extracted with 200 μl of phenol-chloroform-isoamyl alcohol (25:24:1). DNA was precipitated with 3 volumes of ethanol, washed with 70% ethanol, dried, resuspended in sequencing gel loading buffer, and denatured for 5 min at 95°C. Sequencing reaction mixtures that serve as a ladder were prepared with the Sequenase 2.0 DNA sequencing kit (Affymetrix-usb) and primers FP-frag2-HindIII and FP-frag2-XhoI for the top and bottom strands, respectively. After electrophoresis through a denaturing 10% polyacrylamide sequencing gel in 0.8× glycerol-tolerant gel buffer, the gel was dried and detection was carried out with a Phosphor Screen (Kodak) and a Typhoon FLA 9500 imager (GE Healthcare).

RESULTS

CroS is important for the DNA damage-induced activation of SXT transfer. To investigate the role of CroS in the biology of SXT/R391 ICEs, we first monitored the effect of its deletion or overexpression on the transfer of SXT under noninduced conditions and in the presence of the DNA-damaging agent MC. First, we observed that the basal level of SXT transfer remained unaffected by *croS* deletion under noninduced conditions (Fig. 1C). However, while transfer of wild-type SXT was induced more than 30-fold by MC, the Δ*croS* mutant remained virtually unresponsive to MC (Fig. 1D). This phenotype could result from a polar effect of *croS* deletion on the expression of the downstream genes *setCD*, which are part of the same operon. To rule out this possibility, we carried out a complementation assay by expressing *croS* from its native promoter P_L from pSRZ inserted as a single copy into the chromosomal gene *prfC* in a tandem fashion with SXT Δ*croS* (Fig. 1E). pSRZ restored the 30-fold MC-dependent induction to SXT Δ*croS*, thereby confirming that the lack of response to MC exhibited by the Δ*croS* mutant was not due to a polar effect on the expression of *setCD* (Fig. 1D). Moreover, overexpression of *croS* from a P_{BAD} promoter provided by pCroS led to a 10-fold reduction of SXT transfer (Fig. 1C). Altogether, these results suggest that CroS is a crucial regulator for stimulation of SXT transfer in response to DNA damage and suggest the existence of a λ-like SetR-CroS switch in the regulatory network of SXT/R391 ICEs.

Predicted structure and DNA-binding domain of CroS. Extensive studies of many members of the Cro-like family have provided valuable insights for predicting distinctive features of newly discovered Cro-like repressors, which allowed this family to be used as a model in evolutionary studies of protein structure and DNA recognition (42, 43). CroS is predicted to contain a DNA-binding HTH domain (HTH_XRE, COG4197) (Fig. 2A). HHpred analyses revealed that CroS is 25% identical to λ Cro and 35% identical to Xfaso 1, a putative regulator encoded by a prophage of *Xylella fastidiosa*. Although these two homologous regulators have similar regulatory functions and are encoded by genes that are found in similar contexts, λ Cro and Xfaso 1 have been shown to be structurally different. λ Cro is a dimeric protein with a mixed β-sheet/α-helix fold, while Xfaso 1 is a monomeric all-α-helical fold protein in solution (42). A high-accuracy model of the predicted structure of CroS based on the crystal structure of Xfaso 1 was obtained with Phyre2 (44) (Fig. 2B and C). This model suggests that CroS exhibits an all-α structure and exists in solution

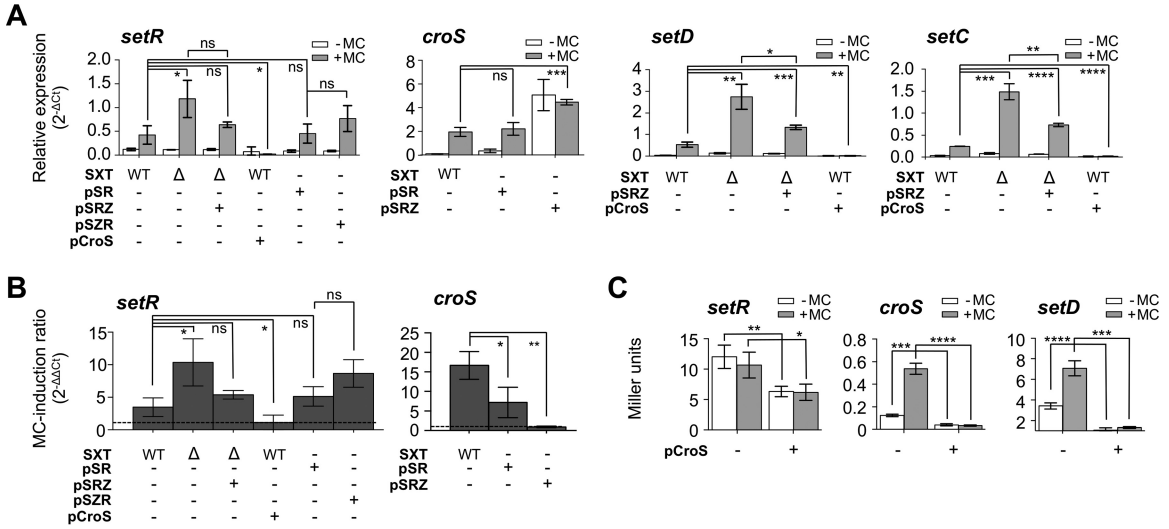

FIG 3 CroS represses expression from P_L and P_R. (A) Effects of *croS* deletion and overexpression on *setR*, *croS*, *setD*, and *setC* mRNA levels. *setR*, *croS*, *setD*, and *setC* mRNA transcript levels in the presence or absence of MC were measured by qRT-PCR. The strains carried SXT (VB17, WT [wild type]) or its Δ*croS* mutant (DPL353, Δ) and/or the simplified pSR (DPL231) construct or its pSZR (DPL241) or pSRZ (DPL263, DPL246) derivative. (B) Effects of *croS* deletion and overexpression on the SOS-dependent induction of *setR* and *croS* expression. The strains used are the same as those in panel A for *setR* and *croS*, but the results are shown as induction ratios obtained by $\Delta\Delta C_T$ calculations. The level of expression without MC was subtracted from the level with MC. The dashed line indicates an MC induction ratio of 1, i.e., no difference between the induced and noninduced conditions. (C) Effect of *croS* overexpression on the translation of *setR*, *croS*, and *setD*. Shown are β-galactosidase assays with strains harboring translational *lacZ* fusions to *setR* (DPL246) and *croS* (DPL241) derived from pSR or to *setD* derived from SXT (DPL297). Each bar represents the mean and standard deviation of values obtained from at least three independent experiments. Statistical analyses of the mean values were performed with two-tailed unpaired *t* tests. Statistical significance is indicated as follows: ns (not significant), $P > 0.05$; *, $P \leq 0.05$; **, $P \leq 0.01$; ***, $P \leq 0.001$; ****, $P \leq 0.0001$.

either as a monomer or as a dimer. Despite extensive similarities, CroS does not contain the cysteine residues C42 and C55 forming the intrasubunit cystine bond observed in Xfaso 1 (42).

We carried out an oligomerization assay with glutaraldehyde cross-linking and observed two bands with sizes compatible to either monomeric or dimeric forms of CroS in solution (Fig. 2D), indicating that CroS can form higher-order complexes even in the absence of target DNA.

CroS acts as a repressor of *setR*. CroS similarity to other Cro-like repressors and the relative positions of *croS* and *setR* led us to hypothesize that the inability of a Δ*croS* mutant to respond to MC induction was at least in part due to the lack of repression of the P_R promoter that drives *setR* expression. To test this hypothesis, we used qRT-PCR to measure and compare the relative mRNA levels of *setR* in wild-type SXT and its Δ*croS* mutant, with or without overexpression of *croS* and in the presence or absence of MC (Fig. 3A and B, *setR*). We observed that while *setR* expression increased only 3-fold upon MC induction in wild-type SXT, it increased 10-fold in the Δ*croS* mutant (Fig. 3A, *setR*). Complementation with pSRZ expressing *croS* from its native promoter restored the induction of *setR* expression to nearly the wild-type level. In contrast, overexpression of *croS* abolished the MC-mediated induction of *setR* expression (Fig. 3B, *setR*). This phenotype results from *croS* overexpression, as control plasmid pCroS-inv, in which the ORF of *croS* is in the reverse orientation, did not lead to abolition of MC-dependent induction (see Fig. S1 in the supplemental material). To isolate the CroS-SetR locus from the rest of the SXT-encoded functions, we also quantified *setR* from pSR to mimic wild-type SXT and from pSZR to mimic SXT Δ*croS*. Although the differences observed were not statistically significant in these simplified genetic contexts, MC-mediated induction of *setR* expression followed trends similar to those observed with complete SXT, suggesting that, besides CroS and SetR, no other ICE-encoded factor regulates *setR* expression (Fig. 3A and B, *setR*). To confirm the repression of *setR* expression by CroS, we also measured the β-galactosidase activity of a *setR′-′lacZ* fusion (pSRZ) in the presence or absence of arabinose-induced pCroS (Fig. 3C, *setR*). Expression of the *setR′-′lacZ* fusion was decreased 2-fold when *croS* was overexpressed. Similar results were obtained regardless of the absence or presence of MC, indicating that *setR* expression is not altered by MC in the absence of the SetR protein. Together, these results confirm that CroS represses *setR*, likely by acting on the P_R promoter.

CroS represses the promoter P_L. In λ, Cro not only represses the expression of the associated *cI* repressor gene but also represses the expression of lytic genes (33). In SXT, integration/excision and conjugative-transfer genes are the counterpart of λ lytic genes. Their expression is activated by the class II transcriptional activator complex SetCD (24, 26). Previously, expression of SetCD was shown to be driven from P_L in the same mRNA transcript that harbors *croS* (30). To assess whether CroS can repress P_L, we measured the relative mRNA level of transcripts containing *setC* and *setD* in cells bearing wild-type SXT or its Δ*croS* mutant derivative in the presence or absence of pSRZ, pCroS, and MC (Fig. 3A, *setD* and *setC*). In an MC-induced Δ*croS* mutant context, we observed that the level of mRNA containing *setD* and *setC* rose 5-fold compared to that of wild-type SXT. This enhanced expression of *setCD* was partially complemented by *croS* provided from its native promoter in pSRZ. Moreover, overexpression of *croS* from pCroS virtually abolished *setD* and *setC* expression (Fig. 3A, *setD* and *setC*). The repressive effect of overexpression of CroS was also observed at the translational level since the *croS′-′lacZ* and *setD′-*

'lacZ fusions yielded very low β-galactosidase activities even when the cells were exposed to MC (Fig. 3C, *croS* and *setD*). Expression of *croS* was similar in the SXT and pSR contexts, while removal of the *setR* gene in pSRZ boosted the expression of *croS*, confirming the repressive function of SetR on P_L (Fig. 3A, *croS*). Abolition of the MC responsiveness in pSRZ confirms the pivotal role of SetR for integration of the SOS signal (RecA*) to the regulatory network. *croS* expressed from its native promoter is not sufficient to completely repress P_L upon MC induction. These expression assays confirm the importance of SetR for the MC-dependent induction of SXT/R391 ICE transfer and that CroS acts as a mild repressor of the P_L promoter, which drives the expression of the master activator complex SetCD.

DNA-binding motif recognized by SetR. To confirm the motif bound by SetR (30), the ~4.8-kb nucleotide sequence overlapping *s084* and *attR* was submitted to the motif-based sequence analysis tool Multiple EM for Motif Elicitation (MEME) (45). This analysis led to the identification of the same operators previously described for SetR located between *croS* and *setR* (OL, O1, O2, and O3), as well as the remote fifth operator O4 (Fig. 4A) (30). A motif alignment and search tool (46) analysis revealed that this motif is not found anywhere else in the SXT sequence.

SetR binding to each independent operator, including O4, was confirmed by EMSAs with purified SetR and a DNA probe corresponding to the single operator (Fig. 4B and C). We observed differential affinities of SetR for its operator sites in the following order: O4 ≈ O1 > O3 > OL > O2. To gain a better understanding of the SetR DNA-binding pattern, we mixed purified SetR with permutated radiolabeled probes, i.e., probes identical in size and partially overlapping each other, containing OL, O1, O2, and O3 (Fig. 4D). SetR binding led to the formation of one predominant complex for all of the probes tested, suggesting that it binds cooperatively to the operators. The variation in the migration distances of the protein-DNA complexes suggests that SetR binding to its operator leads to DNA bending, as shown for other CI-like repressors (47, 48). Indeed, the position of the bending angle along the length of the DNA probe modifies the overall structure of the migrating protein-DNA complex and hence its migration distance (49).

DNA-binding motif recognized by CroS. It has been reported for numerous lambdoid bacteriophages that CI-like and cognate Cro-like repressors have operator sites in common because of similarity in their HTH DNA-binding domains (50–52). The HTH domains of CroS and SetR show 26% identity, which is higher than that of other well-studied λ-like repressor pairs such as λ and P22 (Fig. 4E), suggesting that both proteins have the same operator sites. We tested this hypothesis by carrying out EMSAs with purified CroS and DNA probes corresponding to individual SetR operator sites and confirmed that CroS independently binds to the exact same five operators (Fig. 4C). We observed a differential affinity of CroS for its operator sites in the following order: O3 > OL > O4 > O1 ≈ O2. Like SetR, purified CroS specifically binds P_L and P_R, as neither protein was able to shift probes containing the promoter P_{s089} or P_{s003} in the presence of a specific competitor DNA (annealed oligonucleotides containing either O1 or O2) (see Fig. S2 in the supplemental material). Incubation of purified CroS with permutated radiolabeled probes containing OL, O1, O2, and O3 (Fig. 4D) led to the formation of multiple shifted CroS-DNA complexes, suggesting that, unlike SetR, CroS binds multiple sites in a noncooperative manner. The large footprints observed following CroS binding to the OL, O1, and O2 operators confirm the concomitant binding of CroS to these sites (see Fig. S3 in the supplemental material). Altogether, the results of our SetR and CroS binding assays suggest that both repressors

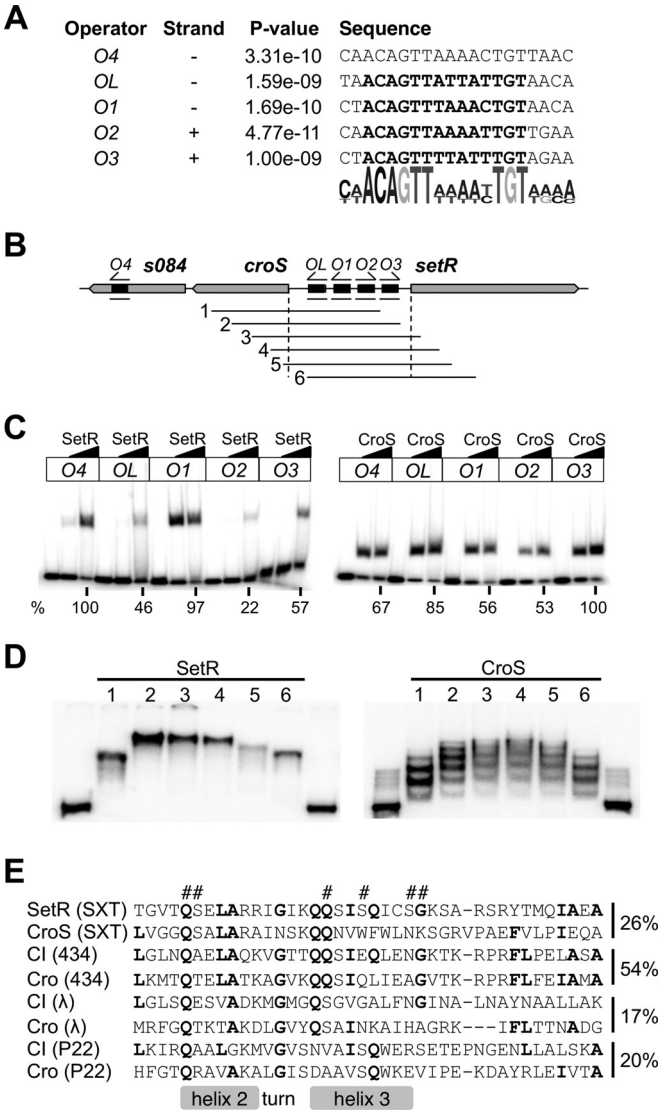

FIG 4 CroS and SetR binding to the switch locus of SXT. (A) Sequences of the five SetR and CroS operators and the associated logo computed by the MEME motif-based sequence analysis tool. The sites previously described by Beaber and Waldor (30) are in bold letters. (B) Representation of the switch locus and the ^{32}P-labeled probes used for the gel shift assays in panels C and D. The orientations of the motifs are indicated above the operators. (C) Binding of 0.6 and 1 μM purified SetR or CroS to annealed oligonucleotides containing a single operator (length of 31 to 36 bp). The leftmost lane for each operator contains the probe alone. The percent intensity of each shifted band in relation to the band with maximal intensity (O4 for SetR and O3 for CroS with 1 μM SetR or CroS) is indicated below the autoradiograph. (D) Bending assays with 1 μM SetR or CroS and permuted PCR probes 1 to 6. The border lanes contain probe 1 with no added protein. (E) Alignment of the HTH_XRE domains (74) of corepressor pairs computed by Clustal Omega (72). Amino acids conserved in at least four of the aligned repressors are in bold. Hash marks (#) above the alignment indicate the specific residues of SetR involved in DNA binding that have been annotated in an NCBI-curated HTH_XRE domain (74). The HTH components are indicated as described elsewhere (51, 75). Percentages of identity between the represented amino acids of the corepressors are indicated on the right of the alignment.

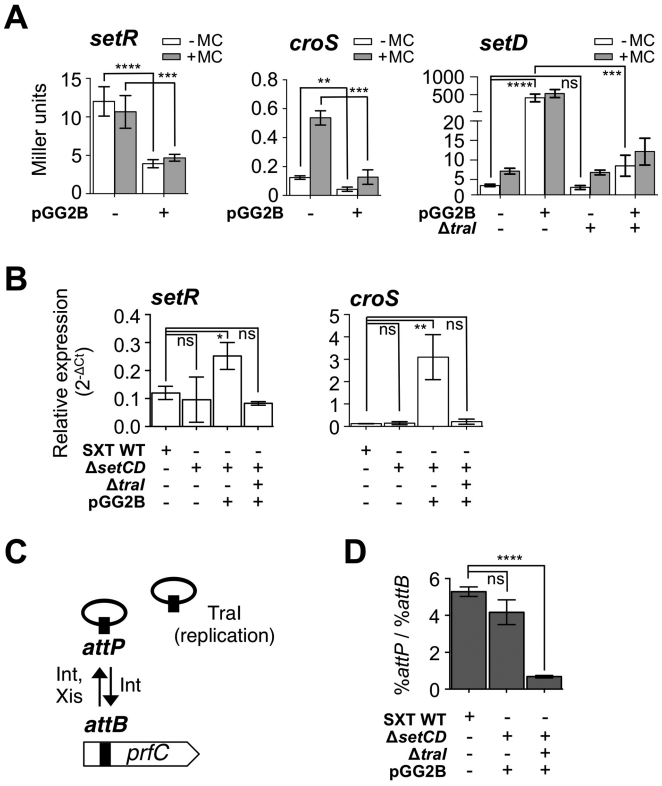

FIG 5 Overexpression of *setCD* leads to an indirect positive feedback loop boosting the expression from P_L and P_R. (A) Effect of SetCD on the expression of *setR*, *croS*, and *setD* translationally fused to *lacZ* measured by β-galactosidase assay in the presence or absence of MC. The strains contain pSRZ (DPL246), pSZR (DPL241), SXT *setD′-′lacZ* Δ*setC* (DPL297), or SXT Δ*traI* *setD′-′lacZ* Δ*setC* (DPL548). Overexpression assays were carried out by expressing *setCD* from the arabinose-inducible P_{BAD} promoter in pGG2B. (B) Effects of *setCD* deletion and overexpression on *setR* and *croS* mRNA levels. qRT-PCR assays were carried out with *E. coli* BW25113 carrying SXT (VB17, WT [wild type]) or its Δ*setCD* or Δ*traI* Δ*setCD* (DPL297 and DPL548) derivative without MC induction. Overexpression assays were carried out by expressing *setCD* from pGG2B. (C) Representation of integration/excision and replication of SXT. (D) Measurement of SXT copy number by qRT-PCR (percent *attP*/percent *attB* with *prfC* as a reference) in SXT derivatives (identical to those in panels A and B) with or without overexpression of *setCD*. Each bar represents the mean and standard deviation of values from three independent experiments. Statistical analyses of the mean values were performed with two-tailed unpaired *t* tests, with the exception of the *setD* results in panel A, for which the logarithms of the mean values were used. Statistical significance is indicated as follows: ns (not significant), $P > 0.05$; *, $P \leq 0.05$; **, $P \leq 0.01$; ***, $P \leq 0.001$; ****, $P \leq 0.0001$.

bind the same operators located in the SXT locus that contains the promoters P_L and P_R.

SetCD indirectly generates a positive feedback loop by activating SXT replication. Previously published work suggests that SetCD regulates its own expression (24). To test this hypothesis, we quantified the β-galactosidase activity of a *setD′-′lacZ* fusion in SXT (DPL297) with or without overexpression of *setCD* from a P_{BAD} promoter (pGG2B) (Fig. 5A, *setD*). Upon overexpression of *setCD*, the β-galactosidase activity of the *setD′-′lacZ* fusion rose by 75-fold. Although *croS* and *setD* are part of the same mRNA transcript driven by P_L (Fig. 5A, *croS*), this drastic increase was not observed for the *setR′-′lacZ* and *croS′-′lacZ* fusions measured from pSRZ (DPL246) and pSZR (DPL241), which are integrated and locked into the chromosome. We also measured the *setR* and *croS* mRNA transcript levels in cells bearing SXT or its Δ*setCD* mutant form in the absence of MC with or without pGG2B (Fig. 5B). Deletion of *setCD* did not significantly alter the expression levels of *setR* and *croS*. In contrast, overexpression of *setCD* increased both *setR* and *croS* mRNA levels, which is seemingly inconsistent with the results obtained by measuring β-galactosidase activities from pSRZ or pSZR (Fig. 5A and B). Altogether, these results suggested that *setCD* expression could be driven from an unidentified alternative SetCD-dependent promoter located between P_L and *setD*. However, despite several attempts, we failed to detect any additional promoter between these two loci with 5′ rapid amplification of cDNA ends (RACE) and primer extension assays (data not shown). Furthermore, genome-wide 5′ RACE and chromatin immunoprecipitation-exonuclease experiments recently confirmed that no promoter is detectable downstream of P_L and that P_L itself is not a SetCD-dependent promoter (26). Another SXT-encoded factor absent from pSZR and pSRZ could explain this discrepancy.

Recent work has established that under inducing conditions, SXT/R391 ICEs replicates by a rolling-circle mechanism initiated by the relaxase TraI. This replication step is important for conjugative transfer, as well as the stability of the ICE in the cell and in the bacterial population (27). To test whether activation of *traI* expression by SetCD (26) is responsible for the increased *setCD* expression in an SXT background, we measured the β-galactosidase activity of the *setD′-′lacZ* fusion in a strain carrying SXT Δ*traI* (DPL548) and pGG2B. We observed that deletion of *traI* abolished the pGG2B-induced increase in *setR*, *croS*, and *setD* expression (Fig. 5A and B). To confirm that *traI* deletion has an effect on the copy number of SXT, we measured the mean copy number of extrachromosomal circular forms of SXT per cell by establishing the ratio of the amount of *attP* recombination sites resulting from SXT excision to the amount of unoccupied chromosomal *attB* sites by real-time qPCR. In theory, each SXT excision event yields one unoccupied *attB* site on the chromosome and one *attP* site on the circular excised SXT if it does not replicate (*attP*/*attB* ratio of 1). Consistent with previous reports (27, 39), the *attP*/*attB* ratio was 5 for wild-type SXT. While this ratio was similar at 4 for SXT Δ*setD′-′lacZ*/pGG2B, it decreased to 0.7 for SXT Δ*traI* *setD′-′lacZ*/pGG2B, confirming the importance of TraI in SXT replication (Fig. 5D). Altogether, these results demonstrate that the apparent involvement of SetCD in the expression of genes in the regulatory region is not due to direct activation of P_L and P_R by SetCD. Instead, SetCD triggers *int*, *xis*, and *traI* expression, thereby driving SXT excision and replication, which increases the copy number of SXT molecules in a larger fraction of the cell population, leading to increased *setR* and *croS-setCD* mRNA levels.

DISCUSSION

SXT/R391 ICEs are major vectors of multidrug resistance dissemination across a plethora of bacterial genera encountered in clinical and environmental settings (7–9). Their highly conserved regulatory region governs the transition between the ICE quiescent and conjugative states (24, 29, 30). Here, we report several new levels of genetic regulation controlling SXT/R391 ICE behavior. Using SXT as a prototypical member of the family, we have identified and characterized the function of CroS, an ICE-encoded Cro-like repressor that serves as a key component of this genetic

switch together with SetR, the main repressor of SXT/R391 ICEs (24). We also show that SetR and CroS are able to bind the O4 operator, likely consolidating the repressed state of these ICEs. Finally, expression of SetCD results in a positive feedback mechanism that is dependent on *traI*, which encodes the presumed relaxase of SXT/R391 ICEs. Given the high conservation of the core genes, especially those of the regulatory region of SXT/R391 ICEs (8), our findings are most likely applicable to all of the members of the family.

The SetR-CroS switch. In λ genetic regulation, the nature of the patterns of CI and Cro binding to the O_R1, O_R2, and O_R3 operators leads either to the activation or repression of *cI* expression from P_{RM} or to the repression or derepression of *cro* from P_R (52). The relative affinities of both repressors for each operator and their respective cell abundance, combined with intrinsic cellular stochasticity, determine the fate of the switch. The closest structural relative of SetR is the CI repressor encoded by lambdoid bacteriophage 434. The N-terminal dimer interface of phage 434 CI was shown to drive the central base preference, which defines the specific affinity of the repressor for each operator independently (53). Even though extensive thermodynamic studies are mandatory to infer quantitative relative affinities, the conditions used in binding reactions allowed us to observe variations in complex formation between the independent operators. With these as an indicators of affinity, the inferred relative affinities of SetR for the five operator sites are O4 ≈ O1 > O3 > OL > O2, which are consistent with what was observed by DNase I footprinting (30). The relative affinities of CroS for the same operators were O3 > OL > O4 > O1 ≈ O2. This binding pattern is consistent with λ Cro, which binds more tightly to O_R3 that to O_R1 and O_R2.

In SXT, the center-to-center O1-O2 and O2-O3 spacings are 24 and 23 bp (Fig. 1B), the ideal distances for cooperative binding, given that two adjacent bound repressor dimers are located on the same side of the DNA helix (54). The OL-O1 spacing of 30 bp suggests that binding of SetR to O1 cannot yield cooperative binding to OL, the orientation of the adjacent repressors being inadequate. Given the observed affinity of SetR, and in agreement with λ regulation, the likely preferred pattern of SetR binding is to O1-O2. The organization of operator sites and promoters of the regulatory locus of SXT (Fig. 1B) suggests that SetR activates its own expression from P_R when cooperatively bound to O1-O2, likely by contacting the σ^{70} subunit of the RNA polymerase (RNAP) (30, 55–57). Binding of SetR to O1-O2 not only triggers its own expression from P_R but also blocks access of the RNAP to P_L, which drives the expression of *setCD* and the subsequent activation of conjugative genes of SXT (26, 29, 30, 58). By analogy with λ *cI* regulation, SetR would repress its own expression by further binding to O3 in addition to O1-O2 when its intracellular level increases (30, 55, 56).

In our assays, the level of SetR translation appeared to be higher than that of CroS translation, suggesting that SetR protein levels are higher than CroS levels (Fig. 3C). In fact, under noninduced conditions, only 1 cell out of 11,500, on average, acts as a donor cell (frequency of exconjugant formation = $8.65 \times 10^{-5} \pm 9.88 \times 10^{-6}$ exconjugant CFU/donor CFU, $n = 3$), suggesting that the quantity of *croS* mRNA transcripts per cell is lower than the quantity of SetR mRNA transcripts in most cells of the population. The primer efficiency bias in qRT-PCR precludes us from directly comparing the amounts of mRNA containing *setR* and *croS* (Fig. 3A). CroS is presumably dominant in only 1 out of 11,500 cells transitioning from the quiescent to the transfer-proficient state of SXT. We have established that CroS is mandatory for SOS induction of SXT transfer, which is consistent with λ regulation (33). CroS represses P_L and P_R when SetR repression is alleviated. This double repression likely delays the recovery of the SetR pool and displaces the balance toward P_L expression long enough for activation of conjugative transfer to occur properly. In our assays, P_L repression by CroS was observed only upon the overexpression of *croS*, not when *croS* was expressed from its native promoter (Fig. 3A, *croS*). This observation suggests that CroS is a weak repressor of P_L. In wild-type induced SXT, conditional replication mediated by TraI (27) increases the *croS* mRNA level (Fig. 5B), which could allow partial repression of P_L. CroS would then act at P_L to mitigate the expression of *setCD*, which has been shown to be toxic when overexpressed (24, 59).

The closest structural relative of CroS is Xfaso 1, a Cro-like repressor whose structure has been determined (42). To our knowledge, experimental data supporting the functionality of Xfaso 1 remain limited (60). Secondary-structure predictions suggest that Xfaso 1 and CroS have an all-α-helix structure, as does the well-studied Cro protein encoded by lambdoid bacteriophage P22 isolated from *Salmonella* (Fig. 2B) (61). The genetic regulation network of P22 is more complex than that of λ, as P22 codes for additional repressors to maintain lysogeny (62). Despite their structural differences (all-α versus α-β folds), Cro proteins likely have highly similar interactions with the P_R and P_{RM} promoters in P22 and λ (63, 64). Indeed, opposite affinities of Cro-like ($O_R3 > O_R1 > O_R2$) and CI-like ($O_R1 > O_R2 > O_R3$) repressors for each operator were observed in both phages. Consistent with our results, the affinity of the Cro-like repressors for each operator exhibits less variation than the affinity of CI-like repressors (63). Study of many natural and synthetic versions of the λ genetic network led to the conclusion that while most components are not essential, altogether they contribute to the overall efficiency and stability of the system (65). We showed that the role of CroS is particularly important in SXT regulation, as SXT lacks two components that are important for noise reduction and stabilization of the λ system, the activator CII and two additional operators in the OL region.

Pleiotropic effect of SetCD overexpression. In λ and in SXT, the *cro* genes are cotranscribed with genes coding for transcriptional activators, *cII* in λ and *setCD* in SXT. These activators are not related. Instead, SetCD is related to FlhCD and AcaCD, the master activators of flagellum synthesis in Gram-negative bacteria (66) and of conjugative transfer functions of IncA/C plasmids (67), respectively. One role of CII is the activation of *cI* by acting at the promoter P_{RE} (52). The intracellular level of CII ultimately makes the decision between lysis and lysogeny. Similarly, our results show that *setR* mRNA levels rise upon *setCD* overexpression (Fig. 5B, *setR*). However, our results revealed that this is not due to direct activation of P_R by SetCD. Instead, expression of *setCD* markedly enhances *int*, *xis*, and *traI* mRNA levels, presumably leading to ICE excision and conjugation-associated replication in a greater portion of the cell population (26, 27). The elevated *setR* and *croS* mRNA levels observed in SetCD-induced bacterial cultures (Fig. 5B) also support this scenario. Paradoxically, overexpression of *setCD* lowered the β-galactosidase activity of the *setR-lacZ* and *croS-lacZ* fusions constructed in the minimal pSR construct (without the SXT backbone) (Fig. 5A). This collateral repressive effect of SetCD overexpression could be caused by ille-

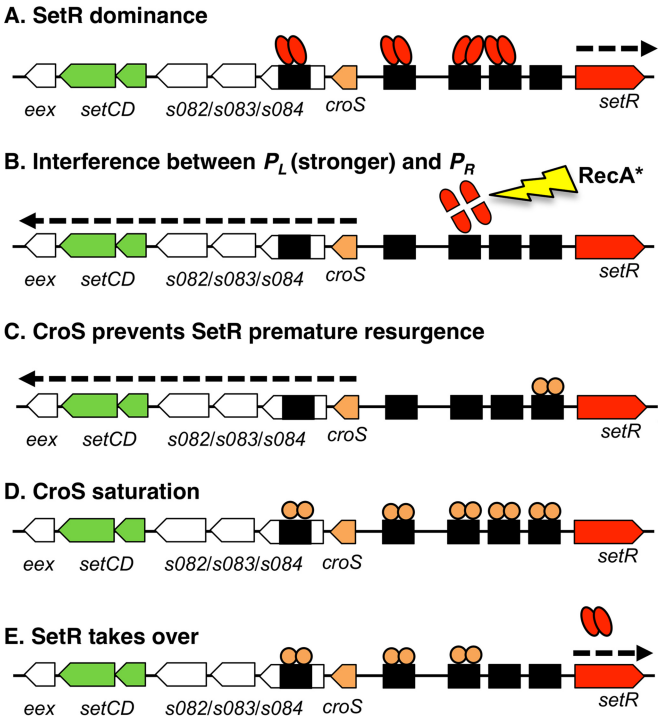

FIG 6 Representation of proposed key intermediate states (A to E) of O4, OL, O1, O2, and O3 binding by SetR or CroS. Panel A is a presumed intermediate of the dominant quiescent behavior, while panels B to E are most likely transient. The dotted arrow indicates active transcription.

gitimate SetCD DNA binding. In addition to being overexpressed, none of the SetCD target promoters was present in such cells to titrate SetCD excess. Alternatively, overexpression of SetCD might reduce *lacZ* expression levels through nonspecific effects on cellular growth rates.

The level of translation was higher for *setD* than for *croS* (Fig. 3C). This difference could be attributable to the spacing between their respective Shine-Dalgarno sequences and start codons, which is closer to the optimum for *setD* than for *croS* (68).

A revised model of SXT early regulation. Since the preferred substrate for RecA*-activated self-cleavage of phage 434 CI is the DNA-bound dimer (69), one could argue that, upon DNA damage, the cooperatively bound SetR-DNA complex becomes the substrate of RecA*, unleashing SetR's latent autoproteolysis activity (29). Release of the operators alleviates the repression exerted by SetR on P_L, allowing *croS* and *setCD* expression (Fig. 6B). CroS, the first translated protein, would bind to O3 to prevent premature resurgence of the SetR pool (Fig. 6C). CroS would then bind in a noncooperative fashion to OL, O1, O2, and O4, thereby preventing adverse overexpression of *setCD* (Fig. 6D). This repression by CroS would allow exclusion of SetR's strong binding to the intergenic region between *croS* and *setR* long enough to observe the SOS-mediated induction of transfer. At some point, CroS would vacate OL, O1, O2, and O3, allowing SetR to take over the intergenic region and reset the quiescent state (Fig. 6E). Our results show that both CroS and SetR are able to bind to O4. Their binding could generate a roadblock that compromises the transcription of the whole *croS-eex* operon driven from P_L beyond O4. Alternatively, because SetR is able to bind cooperatively, its binding could lead to the formation of a long-range loop between a SetR-bound O4 and the intergenic region between *croS* and *setR*. Such a role is unlikely for CroS, which lacks the C-terminal domain mediating self-assembly, cooperative DNA binding, and concomitant loop formation ability (70, 71). This long-range loop or roadblock at O4 mediated by SetR could stabilize the SetR-dominant state. Additional experiments are required to decipher the regulatory mechanism(s) involving the O4 operator site.

The genetic network of SXT/R391 ICEs elegantly sets at play regulatory components reminiscent of lambdoid phages (SetR-CroS epigenetic switch) and bacterial motility (SetCD activation) to rule the propagation of DNA material. The diversity of bacterial hosts in which SXT/R391 ICEs dwell suggests that the regulation system they encode was selected for minimal interactions with host genetic networks apart from their induction stimulated by RecA*. SXT/R391 ICEs take advantage of a host regulatory stress response that can be caused by DNA-targeting antibiotics and UV light to trigger the dissemination of multidrug resistance and other adaptive functions through *Gammaproteobacteria* populations.

ACKNOWLEDGMENTS

This work was supported by a Discovery Grant and Discovery Acceleration Supplement from the Natural Sciences and Engineering Council of Canada (326810 and 412288 to V.B.). V.B. holds a Canada Research Chair in molecular bacterial genetics. D.P.-L. was supported by scholarships from the Fonds de Recherche du Québec.

We are grateful to C. Jouogo Noumsi, V. Côté-Breton, M. Paquette-D'Avignon, D. Ceccarelli, and the Centre de Calcul Scientifique of the Université de Sherbrooke for their technical assistance and to N. Carraro, A. Lavigueur, and J. P. Brousseau for their insightful comments on the manuscript.

REFERENCES

1. **Ramamurthy T, Garg S, Sharma R, Bhattacharya SK, Nair GB, Shimada T, Takeda T, Karasawa T, Kurazano H, Pal A, et al.** 1993. Emergence of novel strain of *Vibrio cholerae* with epidemic potential in southern and eastern India. Lancet **341:**703–704. http://dx.doi.org/10.1016/0140-6736(93)90480-5.
2. **Kaper JB, Morris JG, Jr, Levine MM.** 1995. Cholera. Clin Microbiol Rev **8:**48–86.
3. **Waldor MK, Tschape H, Mekalanos JJ.** 1996. A new type of conjugative transposon encodes resistance to sulfamethoxazole, trimethoprim, and streptomycin in *Vibrio cholerae* O139. J Bacteriol **178:**4157–4165.
4. **Wozniak RA, Waldor MK.** 2010. Integrative and conjugative elements: mosaic mobile genetic elements enabling dynamic lateral gene flow. Nat Rev Microbiol **8:**552–563. http://dx.doi.org/10.1038/nrmicro2382.
5. **Burrus V, Pavlovic G, Decaris B, Guedon G.** 2002. Conjugative transposons: the tip of the iceberg. Mol Microbiol **46:**601–610. http://dx.doi.org/10.1046/j.1365-2958.2002.03191.x.
6. **Hochhut B, Waldor MK.** 1999. Site-specific integration of the conjugal *Vibrio cholerae* SXT element into *prfC*. Mol Microbiol **32:**99–110. http://dx.doi.org/10.1046/j.1365-2958.1999.01330.x.
7. **Spagnoletti M, Ceccarelli D, Rieux A, Fondi M, Taviani E, Fani R, Colombo MM, Colwell RR, Balloux F.** 2014. Acquisition and evolution of SXT-R391 integrative conjugative elements in the seventh-pandemic *Vibrio cholerae* lineage. mBio **5:**e01356-14.
8. **Wozniak RA, Fouts DE, Spagnoletti M, Colombo MM, Ceccarelli D, Garriss G, Dery C, Burrus V, Waldor MK.** 2009. Comparative ICE genomics: insights into the evolution of the SXT/R391 family of ICEs. PLoS Genet **5:**e1000786. http://dx.doi.org/10.1371/journal.pgen.1000786.
9. **Rodríguez-Blanco A, Lemos ML, Osorio CR.** 2012. Integrating conjugative elements as vectors of antibiotic, mercury, and quaternary ammonium compound resistance in marine aquaculture environments. Antimicrob Agents Chemother **56:**2619–2626. http://dx.doi.org/10.1128/AAC.05997-11.
10. **Osorio CR, Marrero J, Wozniak RA, Lemos ML, Burrus V, Waldor MK.**

2008. Genomic and functional analysis of ICE*Pda*SpaI, a fish-pathogen-derived SXT-related integrating conjugative element that can mobilize a virulence plasmid. J Bacteriol **190:**3353–3361. http://dx.doi.org/10.1128/JB.00109-08.

11. **Harada S, Ishii Y, Saga T, Tateda K, Yamaguchi K.** 2010. Chromosomally encoded blaCMY-2 located on a novel SXT/R391-related integrating conjugative element in a *Proteus mirabilis* clinical isolate. Antimicrob Agents Chemother **54:**3545–3550. http://dx.doi.org/10.1128/AAC.00111-10.
12. **López-Pérez M, Gonzaga A, Rodríguez-Valera F.** 2013. Genomic diversity of "deep ecotype" Alteromonas macleodii isolates: evidence for pan-Mediterranean clonal frames. Genome Biol Evol **5:**1220–1232. http://dx.doi.org/10.1093/gbe/evt089.
13. **Badhai J, Kumari P, Krishnan P, Ramamurthy T, Das SK.** 2013. Presence of SXT integrating conjugative element in marine bacteria isolated from the mucus of the coral *Fungia echinata* from Andaman Sea. FEMS Microbiol Lett **338:**118–123. http://dx.doi.org/10.1111/1574-6968.12033.
14. **Pembroke JT, Piterina AV.** 2006. A novel ICE in the genome of *Shewanella putrefaciens* W3-18-1: comparison with the SXT/R391 ICE-like elements. FEMS Microbiol Lett **264:**80–88. http://dx.doi.org/10.1111/j.1574-6968.2006.00452.x.
15. **Coetzee JN, Datta N, Hedges RW.** 1972. R factors from *Proteus rettgeri*. J Gen Microbiol **72:**543–552. http://dx.doi.org/10.1099/00221287-72-3-543.
16. **Beaber JW, Burrus V, Hochhut B, Waldor MK.** 2002. Comparison of SXT and R391, two conjugative integrating elements: definition of a genetic backbone for the mobilization of resistance determinants. Cell Mol Life Sci **59:**2065–2070. http://dx.doi.org/10.1007/s000180200006.
17. **Peters SE, Hobman JL, Strike P, Ritchie DA.** 1991. Novel mercury resistance determinants carried by IncJ plasmids pMERPH and R391. Mol Gen Genet **228:**294–299.
18. **Balado M, Lemos ML, Osorio CR.** 2013. Integrating conjugative elements of the SXT/R391 family from fish-isolated vibrios encode restriction-modification systems that confer resistance to bacteriophages. FEMS Microbiol Ecol **83:**457–467. http://dx.doi.org/10.1111/1574-6941.12007.
19. **Bordeleau E, Brouillette E, Robichaud N, Burrus V.** 2010. Beyond antibiotic resistance: integrating conjugative elements of the SXT/R391 family that encode novel diguanylate cyclases participate to c-di-GMP signalling in *Vibrio cholerae*. Environ Microbiol **12:**510–523. http://dx.doi.org/10.1111/j.1462-2920.2009.02094.x.
20. **Garriss G, Waldor MK, Burrus V.** 2009. Mobile antibiotic resistance encoding elements promote their own diversity. PLoS Genet **5:**e1000775. http://dx.doi.org/10.1371/journal.pgen.1000775.
21. **Kulaeva OI, Wootton JC, Levine AS, Woodgate R.** 1995. Characterization of the *umu*-complementing operon from R391. J Bacteriol **177:**2737–2743.
22. **Hochhut B, Marrero J, Waldor MK.** 2000. Mobilization of plasmids and chromosomal DNA mediated by the SXT element, a constin found in *Vibrio cholerae* O139. J Bacteriol **182:**2043–2047. http://dx.doi.org/10.1128/JB.182.7.2043-2047.2000.
23. **Daccord A, Ceccarelli D, Burrus V.** 2010. Integrating conjugative elements of the SXT/R391 family trigger the excision and drive the mobilization of a new class of *Vibrio* genomic islands. Mol Microbiol **78:**576–588. http://dx.doi.org/10.1111/j.1365-2958.2010.07364.x.
24. **Beaber JW, Hochhut B, Waldor MK.** 2002. Genomic and functional analyses of SXT, an integrating antibiotic resistance gene transfer element derived from *Vibrio cholerae*. J Bacteriol **184:**4259–4269. http://dx.doi.org/10.1128/JB.184.15.4259-4269.2002.
25. **Marrero J, Waldor MK.** 2005. Interactions between inner membrane proteins in donor and recipient cells limit conjugal DNA transfer. Dev Cell **8:**963–970. http://dx.doi.org/10.1016/j.devcel.2005.05.004.
26. **Poulin-Laprade D, Matteau D, Jacques PE, Rodrigue S, Burrus V.** 2015. Transfer activation of SXT/R391 integrative and conjugative elements: unraveling the SetCD regulon. Nucleic Acids Res **43:**2045–2056. http://dx.doi.org/10.1093/nar/gkv071.
27. **Carraro N, Poulin D, Burrus V.** 2015. Replication and active partition of integrative and conjugative elements (ICEs) of the SXT/R391 family: the line between ICEs and conjugative plasmids is getting thinner. PLoS Genet **11:**e1005298. http://dx.doi.org/10.1371/journal.pgen.1005298.
28. **Garriss G, Poulin-Laprade D, Burrus V.** 2013. DNA-damaging agents induce the RecA-independent homologous recombination functions of integrating conjugative elements of the SXT/R391 family. J Bacteriol **195:**1991–2003. http://dx.doi.org/10.1128/JB.02090-12.
29. **Beaber JW, Hochhut B, Waldor MK.** 2004. SOS response promotes horizontal dissemination of antibiotic resistance genes. Nature **427:**72–74. http://dx.doi.org/10.1038/nature02241.
30. **Beaber JW, Waldor MK.** 2004. Identification of operators and promoters that control SXT conjugative transfer. J Bacteriol **186:**5945–5949. http://dx.doi.org/10.1128/JB.186.17.5945-5949.2004.
31. **Svenningsen SL, Costantino N, Court DL, Adhya S.** 2005. On the role of Cro in lambda prophage induction. Proc Natl Acad Sci U S A **102:**4465–4469. http://dx.doi.org/10.1073/pnas.0409839102.
32. **Johnson A, Meyer BJ, Ptashne M.** 1978. Mechanism of action of the cro protein of bacteriophage lambda. Proc Natl Acad Sci U S A **75:**1783–1787. http://dx.doi.org/10.1073/pnas.75.4.1783.
33. **Schubert RA, Dodd IB, Egan JB, Shearwin KE.** 2007. Cro's role in the CI Cro bistable switch is critical for λ's transition from lysogeny to lytic development. Genes Dev **21:**2461–2472. http://dx.doi.org/10.1101/gad.1584907.
34. **Burrus V, Waldor MK.** 2004. Formation of SXT tandem arrays and SXT-R391 hybrids. J Bacteriol **186:**2636–2645. http://dx.doi.org/10.1128/JB.186.9.2636-2645.2004.
35. **Dower WJ, Miller JF, Ragsdale CW.** 1988. High efficiency transformation of *E. coli* by high voltage electroporation. Nucleic Acids Res **16:**6127–6145. http://dx.doi.org/10.1093/nar/16.13.6127.
36. **Demarre G, Guerout AM, Matsumoto-Mashimo C, Rowe-Magnus DA, Marliere P, Mazel D.** 2005. A new family of mobilizable suicide plasmids based on broad host range R388 plasmid (IncW) and RP4 plasmid (IncPalpha) conjugative machineries and their cognate *Escherichia coli* host strains. Res Microbiol **156:**245–255. http://dx.doi.org/10.1016/j.resmic.2004.09.007.
37. **Datsenko KA, Wanner BL.** 2000. One-step inactivation of chromosomal genes in *Escherichia coli* K-12 using PCR products. Proc Natl Acad Sci U S A **97:**6640–6645. http://dx.doi.org/10.1073/pnas.120163297.
38. **Daccord A, Mursell M, Poulin-Laprade D, Burrus V.** 2012. Dynamics of the SetCD-regulated integration and excision of genomic islands mobilized by integrating conjugative elements of the SXT/R391 family. J Bacteriol **194:**5794–5802. http://dx.doi.org/10.1128/JB.01093-12.
39. **Burrus V, Waldor MK.** 2003. Control of SXT integration and excision. J Bacteriol **185:**5045–5054. http://dx.doi.org/10.1128/JB.185.17.5045-5054.2003.
40. **Miller JF.** 1992. A short course in bacterial genetics. Cold Spring Harbor Laboratory Press, Plainview, NY.
41. **Pradervand N, Delavat F, Sulser S, Miyazaki R, van der Meer JR.** 2014. The TetR-type MfsR protein of the integrative and conjugative element (ICE) ICEclc controls both a putative efflux system and initiation of ICE transfer. J Bacteriol **196:**3971–3979. http://dx.doi.org/10.1128/JB.02129-14.
42. **Roessler CG, Hall BM, Anderson WJ, Ingram WM, Roberts SA, Montfort WR, Cordes MH.** 2008. Transitive homology-guided structural studies lead to discovery of Cro proteins with 40% sequence identity but different folds. Proc Natl Acad Sci U S A **105:**2343–2348. http://dx.doi.org/10.1073/pnas.0711589105.
43. **Hall BM, Lefevre KR, Cordes MH.** 2005. Sequence correlations between Cro recognition helices and cognate O(R) consensus half-sites suggest conserved rules of protein-DNA recognition. J Mol Biol **350:**667–681. http://dx.doi.org/10.1016/j.jmb.2005.05.025.
44. **Kelley LA, Sternberg MJ.** 2009. Protein structure prediction on the Web: a case study using the Phyre server. Nat Protoc **4:**363–371. http://dx.doi.org/10.1038/nprot.2009.2.
45. **Bailey TL, Elkan C.** 1994. Fitting a mixture model by expectation maximization to discover motifs in biopolymers. Proc Int Conf Intell Syst Mol Biol **2:**28–36.
46. **Bailey TL, Gribskov M.** 1998. Combining evidence using p-values: application to sequence homology searches. Bioinformatics **14:**48–54. http://dx.doi.org/10.1093/bioinformatics/14.1.48.
47. **Griffith J, Hochschild A, Ptashne M.** 1986. DNA loops induced by cooperative binding of lambda repressor. Nature **322:**750–752. http://dx.doi.org/10.1038/322750a0.
48. **Koudelka GB.** 1991. Bending of synthetic bacteriophage 434 operators by bacteriophage 434 proteins. Nucleic Acids Res **19:**4115–4119. http://dx.doi.org/10.1093/nar/19.15.4115.
49. **Kim J, Zwieb C, Wu C, Adhya S.** 1989. Bending of DNA by gene-regulatory proteins: construction and use of a DNA bending vector. Gene **85:**15–23. http://dx.doi.org/10.1016/0378-1119(89)90459-9.

50. **Koudelka GB, Lam CY.** 1993. Differential recognition of OR1 and OR3 by bacteriophage 434 repressor and Cro. J Biol Chem **268:**23812–23817.
51. **Sauer RT, Yocum RR, Doolittle RF, Lewis M, Pabo CO.** 1982. Homology among DNA-binding proteins suggests use of a conserved super-secondary structure. Nature **298:**447–451. http://dx.doi.org/10.1038/298447a0.
52. **Ptashne M.** 2004. A genetic switch: phage lambda revisited, 3rd ed. Cold Spring Harbor Laboratory Press, Cold Spring Harbor, NY.
53. **Koudelka GB.** 1998. Recognition of DNA structure by 434 repressor. Nucleic Acids Res **26:**669–675. http://dx.doi.org/10.1093/nar/26.2.669.
54. **Mao C, Carlson NG, Little JW.** 1994. Cooperative DNA-protein interactions. Effects of changing the spacing between adjacent binding sites. J Mol Biol **235:**532–544.
55. **Li M, Moyle H, Susskind MM.** 1994. Target of the transcriptional activation function of phage lambda cI protein. Science **263:**75–77. http://dx.doi.org/10.1126/science.8272867.
56. **Xu J, Koudelka GB.** 2000. DNA sequence requirements for the activation of 434 P(RM) transcription by 434 repressor. DNA Cell Biol **19:**621–630. http://dx.doi.org/10.1089/104454900750019380.
57. **Kuldell N, Hochschild A.** 1994. Amino acid substitutions in the −35 recognition motif of sigma 70 that result in defects in phage lambda repressor-stimulated transcription. J Bacteriol **176:**2991–2998.
58. **Meyer BJ, Maurer R, Ptashne M.** 1980. Gene regulation at the right operator (OR) of bacteriophage lambda. II. OR1, OR2, and OR3: their roles in mediating the effects of repressor and cro. J Mol Biol **139:**163–194.
59. **Armshaw P, Pembroke JT.** 2013. Generation and analysis of an ICE R391 deletion library identifies genes involved in the element encoded UV-inducible cell-sensitising function. FEMS Microbiol Lett **342:**45–53. http://dx.doi.org/10.1111/1574-6968.12107.
60. **de Mello Varani A, Souza RC, Nakaya HI, de Lima WC, Paula de Almeida LG, Kitajima EW, Chen J, Civerolo E, Vasconcelos AT, Van Sluys MA.** 2008. Origins of the *Xylella fastidiosa* prophage-like regions and their impact in genome differentiation. PLoS One **3:**e4059. http://dx.doi.org/10.1371/journal.pone.0004059.
61. **Newlove T, Konieczka JH, Cordes MH.** 2004. Secondary structure switching in Cro protein evolution. Structure **12:**569–581. http://dx.doi.org/10.1016/j.str.2004.02.024.
62. **Susskind MM, Botstein D.** 1978. Molecular genetics of bacteriophage P22. Microbiol Rev **42:**385–413.
63. **Poteete AR, Hehir K, Sauer RT.** 1986. Bacteriophage P22 Cro protein: sequence, purification, and properties. Biochemistry **25:**251–256. http://dx.doi.org/10.1021/bi00349a035.
64. **Poteete AR, Ptashne M.** 1982. Control of transcription by the bacteriophage P22 repressor. J Mol Biol **157:**21–48. http://dx.doi.org/10.1016/0022-2836(82)90511-3.
65. **Little JW.** 2010. Evolution of complex gene regulatory circuits by addition of refinements. Curr Biol **20:**R724-734. http://dx.doi.org/10.1016/j.cub.2010.06.028.
66. **Soutourina OA, Bertin PN.** 2003. Regulation cascade of flagellar expression in Gram-negative bacteria. FEMS Microbiol Rev **27:**505–523. http://dx.doi.org/10.1016/S0168-6445(03)00064-0.
67. **Carraro N, Matteau D, Luo P, Rodrigue S, Burrus V.** 2014. The master activator of IncA/C conjugative plasmids stimulates genomic islands and multidrug resistance dissemination. PLoS Genet **10:**e1004714. http://dx.doi.org/10.1371/journal.pgen.1004714.
68. **Chen H, Bjerknes M, Kumar R, Jay E.** 1994. Determination of the optimal aligned spacing between the Shine-Dalgarno sequence and the translation initiation codon of Escherichia coli mRNAs. Nucleic Acids Res **22:**4953–4957. http://dx.doi.org/10.1093/nar/22.23.4953.
69. **Pawlowski DR, Koudelka GB.** 2004. The preferred substrate for RecA-mediated cleavage of bacteriophage 434 repressor is the DNA-bound dimer. J Bacteriol **186:**1–7. http://dx.doi.org/10.1128/JB.186.1.1-7.2004.
70. **Bell CE, Frescura P, Hochschild A, Lewis M.** 2000. Crystal structure of the lambda repressor C-terminal domain provides a model for cooperative operator binding. Cell **101:**801–811. http://dx.doi.org/10.1016/S0092-8674(00)80891-0.
71. **Bell CE, Lewis M.** 2001. Crystal structure of the lambda repressor C-terminal domain octamer. J Mol Biol **314:**1127–1136. http://dx.doi.org/10.1006/jmbi.2000.5196.
72. **Sievers F, Wilm A, Dineen D, Gibson TJ, Karplus K, Li W, López R, McWilliam H, Remmert M, Soding J, Thompson JD, Higgins DG.** 2011. Fast, scalable generation of high-quality protein multiple sequence alignments using Clustal Omega. Mol Syst Biol **7:**539.
73. **Dodd IB, Egan JB.** 1990. Improved detection of helix-turn-helix DNA-binding motifs in protein sequences. Nucleic Acids Res **18:**5019–5026. http://dx.doi.org/10.1093/nar/18.17.5019.
74. **Marchler-Bauer A, Zheng C, Chitsaz F, Derbyshire MK, Geer LY, Geer RC, Gonzales NR, Gwadz M, Hurwitz DI, Lanczycki CJ, Lu F, Lu S, Marchler GH, Song JS, Thanki N, Yamashita RA, Zhang D, Bryant SH.** 2013. CDD: conserved domains and protein three-dimensional structure. Nucleic Acids Res **41:**D348-352. http://dx.doi.org/10.1093/nar/gks1243.
75. **Harrison SC, Aggarwal AK.** 1990. DNA recognition by proteins with the helix-turn-helix motif. Annu Rev Biochem **59:**933–969. http://dx.doi.org/10.1146/annurev.bi.59.070190.004441.
76. **Singer M, Baker TA, Schnitzler G, Deischel SM, Goel M, Dove W, Jaacks KJ, Grossman AD, Erickson JW, Gross CA.** 1989. A collection of strains containing genetically linked alternating antibiotic resistance elements for genetic mapping of *Escherichia coli*. Microbiol Rev **53:**1–24.
77. **Grenier F, Matteau D, Baby V, Rodrigue S.** 2014. Complete genome sequence of *Escherichia coli* BW25113. Genome Announc **2:**e01038-14.
78. **Ceccarelli D, Daccord A, Rene M, Burrus V.** 2008. Identification of the origin of transfer (*oriT*) and a new gene required for mobilization of the SXT/R391 family of integrating conjugative elements. J Bacteriol **190:**5328–5338. http://dx.doi.org/10.1128/JB.00150-08.
79. **Guzman LM, Belin D, Carson MJ, Beckwith J.** 1995. Tight regulation, modulation, and high-level expression by vectors containing the arabinose P_{BAD} promoter. J Bacteriol **177:**4121–4130.
80. **Miller H.** 1987. Practical aspects of preparing phage and plasmid DNA: growth, maintenance, and storage of bacteria and bacteriophage. Methods Enzymol **152:**145–170. http://dx.doi.org/10.1016/0076-6879(87)52016-X.